Assessment of Standard Force Field Models Against High-Quality *Ab Initio* Potential Curves for Prototypes of π–π, CH/π, and SH/π Interactions*

C. DAVID SHERRILL,[1] BOBBY G. SUMPTER,[2,3] MUTASEM O. SINNOKROT,[4] MICHAEL S. MARSHALL,[1] EDWARD G. HOHENSTEIN,[1] ROSS C. WALKER,[5] IAN R. GOULD[6]

[1] *Center for Computational Molecular Science and Technology, School of Chemistry and Biochemistry, Georgia Institute of Technology, Atlanta, Georgia 30332-0400*

[2] *Computer Science and Mathematics Division, Oak Ridge National Laboratory, Oak Ridge, Tennessee 37831*

[3] *Center for Nanophase Materials Sciences, Oak Ridge National Laboratory, Oak Ridge, Tennessee 37831*

[4] *Department of Chemistry, Faculty of Science, University of Jordan, Amman 11942, Jordan*

[5] *San Diego Supercomputer Center, University of California San Diego, La Jolla, California 92093-0505*

[6] *Department of Chemistry, Imperial College London, London SW7 2AZ, United Kingdom*

Received 9 August 2008; Revised 19 December 2008; Accepted 31 December 2008
DOI 10.1002/jcc.21226
Published online 25 February 2009 in Wiley InterScience (www.interscience.wiley.com).

Abstract: Several popular force fields, namely, CHARMM, AMBER, OPLS-AA, and MM3, have been tested for their ability to reproduce highly accurate quantum mechanical potential energy curves for noncovalent interactions in the benzene dimer, the benzene-CH_4 complex, and the benzene-H_2S complex. All of the force fields are semi-quantitatively correct, but none of them is consistently reliable quantitatively. Re-optimization of Lennard-Jones parameters and symmetry-adapted perturbation theory analysis for the benzene dimer suggests that better agreement cannot be expected unless more flexible functional forms (particularly for the electrostatic contributions) are employed for the empirical force fields.

 J Comput Chem 30: 2187–2193, 2009

Key words: quantum chemistry; electronic structure; coupled cluster theory; molecular mechanics; computational chemistry

Introduction

Non bonded interactions govern supramolecular chemistry, molecular recognition, drug binding,[1–3] and they are critical for understanding the structure of biomolecules or organic crystals.[4–8] However, despite their importance, the nature of many of the prototype noncovalent interactions remains poorly understood.[9] For example, although the very popular Hunter-Sanders model of π–π interactions holds that geometric and substituent effects can be understood solely on the basis of changes in electrostatic interactions,[10] recent quantum-mechanical studies suggest that differential dispersion effects are also critical and cannot be ignored.[11–13] Fortunately, symmetry-adapted perturbation theory analysis[14] of a limited number of prototype van der Waals dimers suggests that induction terms (such as dipole/induced dipole, etc.) are relatively minor for non-covalent interactions involving aromatic π systems, and the dominant factors are electrostatics, exchange-repulsion, and dispersion.[12,13,15,16] This suggests that standard force fields with point-charge electrostatics[17] may be capable of providing reliable results for such interactions. Fortunately, the recent publication of

*This work is dedicated in memory of Tamer Sinnokrot.

Correspondence to: C. D. Sherrill; e-mail: sherrill@gatech.edu

Contract/grant sponsor: National Science Foundation; contract/grant number: CHE-0715268

Contract/grant sponsor: CRIF; contract/grant number: CHE-04-43564

Contract/grant sponsor: Petroleum Research Fund of the ACS; contract/grant number: 44262-AC6

Contract/grant sponsor: Division of Scientific User Facilities, U.S. Department of Energy

Contract/grant sponsor: SDSC Strategic Applications Collaborations program and National Science Foundation; contract/grant number: 0438741

several benchmark-quality quantum-mechanical potential energy curves for prototypical non-bonded π-interactions[15,16,18–20] now makes it possible to directly assess the reliability of standard force fields for these interactions.

Although force field parameters are often obtained by fitting to quantum mechanical data, typically the quantum computations have been performed at a low level of theory (e.g., Hartree-Fock with a small basis set, or occasionally second-order perturbation theory with a modest basis set). There have been some limited comparisons in the literature to higher-quality data,[21–23] but we are unaware of any previous systematic comparison for entire potential energy curves. In this work, we compare several popular force fields against quantum mechanical results obtained near the *ab initio* limit for several prototypes of non-bonded interactions, namely, three configurations of the benzene dimer (π–π interactions), CH_4-benzene (C–H/π), and H_2S-benzene (S–H/π).

Although larger prototype systems might provide more realistic models of noncovalent interactions in biomolecules, unfortunately it becomes much harder to obtain benchmark-quality *ab initio* results for them. Nevertheless, the models used here appear to be sufficient to capture the basic physics of relevant noncovalent interactions. In previous work, we found that the behavior of the H_2S-benzene complex is surprisingly similar to that of methanethiol-benzene.[24] Moreover, the most frequent contact distance for C–H/π interactions in peptide crystal structures is the same as the equilibrium distance in CH_4-benzene,[15] and the geometric preferences of H_2S-benzene are those statistically observed in the Protein Data Bank.[24]

It is important to point out that many force fields are fit not only to *ab initio* data, but also to experimental thermodynamic properties of liquids.[25] Hence, imperfect agreement with *ab initio* data for gas-phase dimers is not necessarily a sign that a force field is inaccurate in condensed phase simulations, because in principle the errors in the dimer potential can partially cancel errors due to the lack of explicit electron polarization in most force fields. Indeed, the AMBER FF99 force field[26] deliberately uses lower-level Hartree-Fock/6-31G* quantum computations to derive atomic charges because this approach tends to overestimate molecular polarity, and such errors appear to partially cancel the lack of polarization in the standard force fields (many nonpolarizable water models have dipole moments about 20% larger than for gas-phase water, but they yield good condensed-phase properties).[26] These considerations notwithstanding, we believe comparison to high-level quantum data for gas-phase dimers remains valuable as part of a broader effort to develop next-generation polarizable force fields which aspire to model both gas-phase and condensed phase systems. Indeed, apart from such comparisons, there is no clear path forward for producing more accurate force fields appropriate for a wide variety of chemical systems and conditions. In the present work, our analysis demonstrates deficiencies in the standard atom-centered point-charge electrostatic model for systems involving π–π interactions; proper modeling of such interactions would appear to require a description of charge interpenetration effects.

Theoretical Methods

Here we compare the following standard force fields: AMBER,[27] CHARMM,[28] OPLS,[25,29,30] and MM3.[31] AMBER and CHARMM are widely used for modeling proteins and nucleic acids. Semiempirical methods are also briefly considered; as an example, we examine Jorgensen's pairwise distance directed Gaussian (PDDG) modification[32] of the PM3 semiempirical method,[33] as implemented in AMBER.[34] These approaches are benchmarked against estimated coupled-cluster singles, doubles, and perturbative triples [CCSD(T)] results in the complete basis set (CBS) limit for the benzene dimer (Takatani et al., manuscript in preparation), CH_4-benzene,[15] and H_2S-benzene.[16]

The classical, nonpolarizable AMBER force field has the following form:[26,27,35]

$$V = \sum_{\text{bonds}} K_r(r - r_{\text{eq}})^2 + \sum_{\text{angles}} K_\theta(\theta - \theta_{\text{eq}})^2 + \frac{1}{2}\sum_{\text{dihedrals}} V_n[1 + \cos(n\phi - \gamma)] + \sum_{i<j}^{\text{nonbond}} \left(\frac{A_{ij}}{R_{ij}^{12}} - \frac{B_{ij}}{R_{ij}^{6}} + \frac{q_i q_j}{\epsilon R_{ij}}\right), \quad (1)$$

where stretches and bends are treated with only quadratic terms, torsional angles use a Fourier expansion, and van der Waals terms use a Lennard-Jones expression. The nonbond terms exclude all 1-2 (bond), 1-3 (angle) interactions, whereas 1-4 (dihedral) van der Waals interactions are divided by 2.0 and 1-4 electrostatic interactions divided by 1.2. The original force field also included an explicit 10-12 function for hydrogen bonds, but subsequent improvements in the electrostatic and van der Waals parameters[26,35] allowed for an adequate treatment of H-bonds without the use of this additional 10-12 term in the force field. In this work, we used the AMBER FF99 version of this force field.[26] Charges were fit using the restrained electrostatic potential (RESP) approach,[26] following the procedure developed for the FF99 force field. This involved optimization using MP2/6-31G* followed by an HF/6-31G* single point computation to evaluate the electrostatic potential. This was then fitted to atom centered point charges in a two state RESP fit. This yields $q(H) = -q(C) = 0.127748$ a.u. for benzene. For H_2S, $q(S) = -0.358981$, and for CH_4, $q(C) = -0.278946$. AMBER atom types are HA and CA for benzene; SH and HS for H_2S; and CT and HC for methane. Although other AMBER force fields are also available, they typically employ the same van der Waals parameters as FF99, and they generally use similar charge fitting procedures.

The optimized potential for liquid simulations all-atom (OPLS-AA) force field[25,29,30] takes the stretching, bending, and torsional terms from AMBER but refines the nonbonded interactions by adjusting the parameters to reproduce quantities such as the experimental densities and heats of vaporization of liquids. Torsional terms are fit to Hartree-Fock[25] or MP2[30] results for small molecules. Explicit terms for hydrogen bonding are not included, and no additional interaction sites are employed for lone pairs. In this study, we used charges optimized for benzene, $q(H) = -q(C) = 0.115$, as reported by Jorgensen and Severance.[36] As obtained by Tinker 4.2,[37–39] for methane, $q(C) = -0.24$, and for H_2S, $q(S) = -0.47$.

The all-atom CHARMM force field[28,40,41] has a similar functional form to the AMBER force field discussed earlier, although

it adds a "Urey-Bradley" term for 1-3 interactions and treats "improper torsions" with a special term. In this work, we used the CHARMM27 force field.[41,42] The CHARMM force field expresses the Lennard-Jones term as

$$E_{\mathrm{VDW}} = \sum_{i<j}^{\mathrm{nonbond}} \epsilon_{ij} \left[\left(\frac{R_{ij}^0}{R_{ij}} \right)^{12} - 2 \left(\frac{R_{ij}^0}{R_{ij}} \right)^{6} \right], \qquad (2)$$

where the energy parameter ϵ_{ij} is based on the geometric mean of ϵ_i and ϵ_j (deduced from homonuclear potentials for atoms i and j, respectively), and R_{ij}^0 is based on the arithmetic mean of R_i^0 and R_j^0. This Lennard-Jones functional form is mathematically equivalent to the one used by AMBER. The CHARMM nonbonded parameters for benzene are the same as those in OPLS-AA. Partial charges for the simple molecules CH_4 and H_2S are not available as part of the CHARMM force field specification, and the procedure used to obtain charges when the CHARMM27 parameters were developed is rather complex.[42] Hence, we have employed the OPLS-AA partial charges for CH_4 and H_2S.* The Lennard-Jones parameters are, however, different between CHARMM27 and OPLS-AA for these atoms.

The MM3 force field[31] is considerably more complex than those discussed earlier. It employs higher (up to quartic) powers of bond stretches and angle bends and also includes cross terms such as stretch-bend, torsion-stretch, and torsion-bend interactions. However, for our present purposes, the nonbonded interactions are the ones that are pertinent. The van der Waals term in MM3 is expressed as

$$E_{\mathrm{vdw}} = \sum_{i<j}^{\mathrm{nonbond}} \epsilon_{ij} \left[-2.25 \left(R_{ij}^0 / R_{ij} \right)^6 + 1.84 \times 10^5 e^{-12.0 \left(R_{ij}/R_{ij}^0 \right)} \right]. \qquad (3)$$

The van der Waals term in MM3 was made somewhat less repulsive at short distances than that in its predecessor, MM2. Like MM2 but unlike the force fields previously discussed, MM3 represents the charge distribution for a neutral molecule by bond dipoles rather than by atom-centered point charges; the electrostatic energy is evaluated as the sum of the dipole-dipole interactions. Aliphatic C–C and C–H bonds are not assigned dipole moments. However, MM3 does include bond dipole moments for aromatic C–H bonds; as noted by Allinger, Yuh, and Lii,[31] "in the case of benzene, it is clear that one must have charges on the hydrogens and carbons if one is to reproduce the crystal structure, the stability of the perpendicular benzene dimer, and related facts."

AMBER results were obtained using AMBER version 9.[43] Tinker version 4.2[37–39] was used to obtain the OPLS, MM3, and CHARMM results.† For the benzene dimer, results were also checked against a new module, NONBONDED, added to the PSI3 program package[44] for this and future studies.

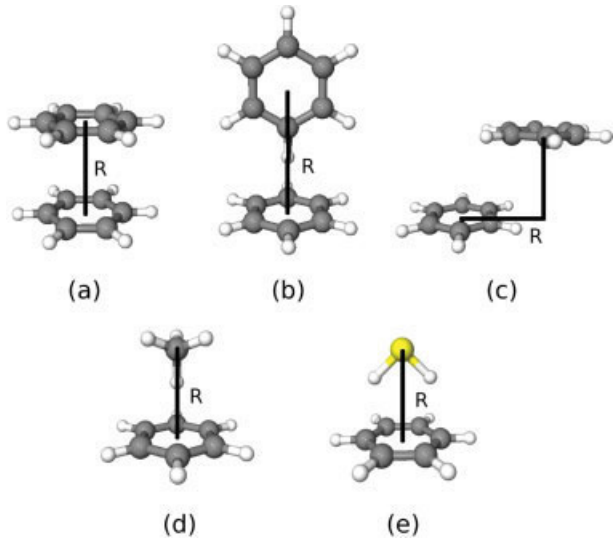

Figure 1. Configurations studied for various prototypes of nonbonded interactions. Lines indicate the intermolecular distances varied; monomer geometries were frozen. [Color figure can be viewed in the online issue, which is available at www.interscience.wiley.com.]

Results and Discussion

Figure 1 presents the chemical systems considered and the distances varied in generating potential energy curves. Let us first consider results for various prototype configurations of the benzene dimer, namely, the sandwich, T-shaped, and parallel-displaced configurations. Potential energy curves (using fixed monomer geometries) are presented in Figures 2–6. For the parallel-displaced configurations, interaction energies are plotted against the horizontal displacement as the vertical separation between the rings is fixed at 3.2 (Fig. 4), 3.4 (Fig. 5), and 3.6 Angstrom (Fig. 6). For the sandwich configuration only (Fig. 2), we have included semiempirical results using the PDDG/PM3 model.[32,33] Being approximations to Hartree-Fock theory, standard semiempirical methods lack any description of long-range correlation effects and are thus unsuitable for modeling noncovalent interactions. The PDDG/PM3 potential curve for the benzene dimer in Figure 2 is completely wrong qualitatively, demonstrating no attraction between the benzene rings. Similar results can be expected for any Hartree-Fock or semiempirical approach which has not been corrected with some model of dispersion interactions.

In contrast to the semiempirical results, all of the empirical approaches are at least qualitatively correct for the sandwich and T-shaped (Fig. 3) configurations, although all of the standard empirical methods under-bind the T-shaped configuration and are too

*Note also that when using Tinker 4.2 with the CHARMM27 force field, the assignment of atom types atom types CT3 and HA for CH_4 and HS and S for H_2S does not lead to neutral molecules when the default charges for these atom types are employed. This is another reason we chose to set the atomic charges to their OPLS-AA values.

†When other programs such as Hyperchem are used, somewhat different results may be obtained due to variations in the details of the implementation. However, such variations do not change any of our conclusions qualitatively.

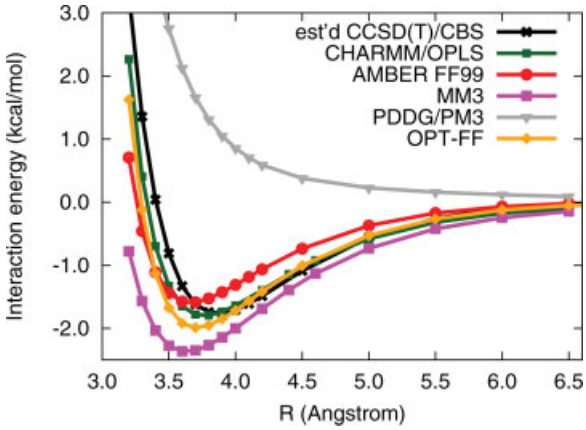

Figure 2. Interaction energy (kcal mol^{-1}) for the sandwich benzene dimer. OPT-FF denotes a force field with Lennard-Jones parameters optimized for the benzene dimer. Benchmark coupled-cluster data from Takatani et al. (manuscript in preparation).

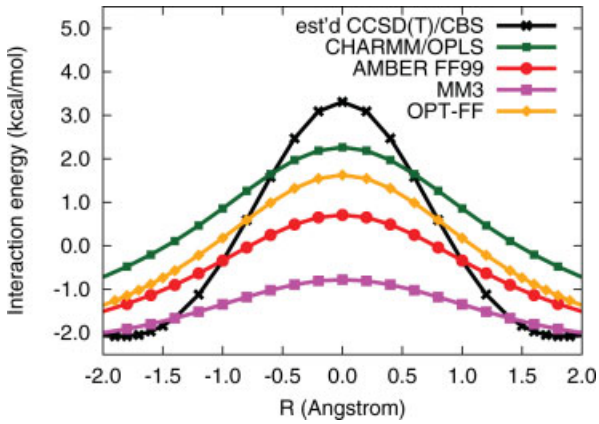

Figure 4. Interaction energy (kcal mol^{-1}) for the parallel-displaced benzene dimer with a vertical interplanar separation of 3.2 Å. OPT-FF denotes a force field with Lennard-Jones parameters optimized for the benzene dimer. Benchmark coupled-cluster data from Takatani et al. (manuscript in preparation).

repulsive at short intermonomer distances. For the parallel-displaced configurations in Figures 4–6, empirical methods show more significant deviations from the quantum-mechanical benchmarks. The empirical curves are too flat; the energies are too attractive at small horizontal displacements, and they are not attractive enough at large horizontal displacements. The agreement between force fields and quantum mechanics for this case can only be considered very rough.

For the sandwich and parallel-displaced configurations, MM3 provides the most attractive potentials. For the sandwich, it overbinds compared to the quantum data. For the parallel-displaced configurations, it remains somewhat under-bound at large horizontal displacements, but it shows the largest over-binding at short horizontal displacements. Overall, MM3 shows the worst agreement with the benchmark results for the sandwich and parallel-displaced configurations. It also performs worst among force fields considered for the T-shaped configuration, although in this case it underbinds rather than overbinds. AMBER improves over MM3 for these test cases, although its potential curve is shifted toward shorter intermonomer separations for the sandwich configuration, and the potential curves for the parallel displaced configurations remain too shallow. For the T-shaped configuration, the AMBER curve is nearly coincident with those from CHARMM and OPLS.

Overall the best match to the quantum data for the benzene dimer is found for CHARMM and OPLS (which are identical for the benzene dimer). The agreement for the sandwich configuration is quite good. For the parallel-displaced configurations, CHARMM and OPLS underbind at larger horizontal displacements, but they provide approximately the correct interaction energy at the top of the barrier, and they provide the best match of the force fields considered to the curvature of the quantum potential. Like AMBER and MM3,

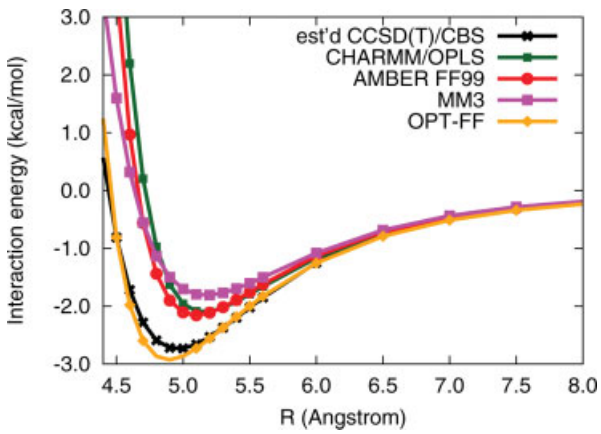

Figure 3. Interaction energy (kcal mol^{-1}) for the T-shaped benzene dimer. OPT-FF denotes a force field with Lennard-Jones parameters optimized for the benzene dimer. Benchmark coupled-cluster data from Takatani et al. (manuscript in preparation).

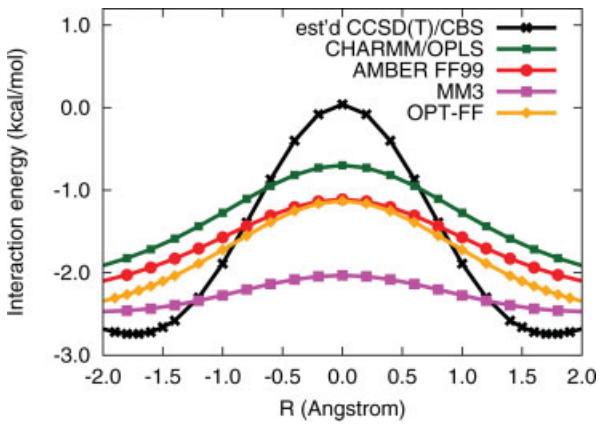

Figure 5. Interaction energy (kcal mol^{-1}) for the parallel-displaced benzene dimer with a vertical interplanar separation of 3.4 Å. OPT-FF denotes a force field with Lennard-Jones parameters optimized for the benzene dimer. Benchmark coupled-cluster data from Takatani et al. (manuscript in preparation).

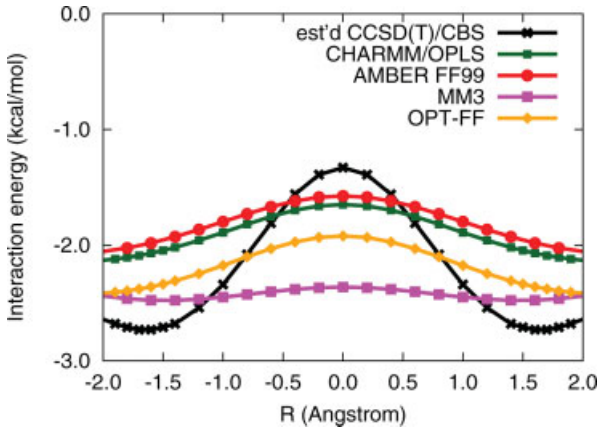

Figure 6. Interaction energy (kcal mol^{-1}) for the parallel-displaced benzene dimer with a vertical interplanar separation of 3.6 Å. OPT-FF denotes a force field with Lennard-Jones parameters optimized for the benzene dimer. Benchmark coupled-cluster data from Takatani et al. (manuscript in preparation).

unfortunately CHARMM and OPLS are somewhat underbound for the T-shaped configuration.

Results for the methane–benzene test case are presented in Figure 7. Unlike the sandwich or parallel-displaced benzene dimers, but like the T-shaped benzene dimer, now MM3 is slightly underbound. AMBER, OPLS, and CHARMM provide nearly identical results and are also all underbound compared to the benchmark results. All curves are in agreement beyond about 5 Å. The maximum binding energies along the curves are 1.06 (CHARMM), 1.07 (AMBER), 1.06 (OPLS), 0.87 (MM3), and 1.47 kcal mol^{-1} for CCSD(T)/CBS.

For the case of H_2S-benzene (Fig. 8), the empirical potentials are not quite repulsive enough at short intermolecular separations. CHARMM, which had been among the better performers for the other tests, is now the worst, leading to significant overestimation of the attraction near equilibrium. AMBER, MM3, and OPLS provide reasonable interaction energies, but their minima are displaced

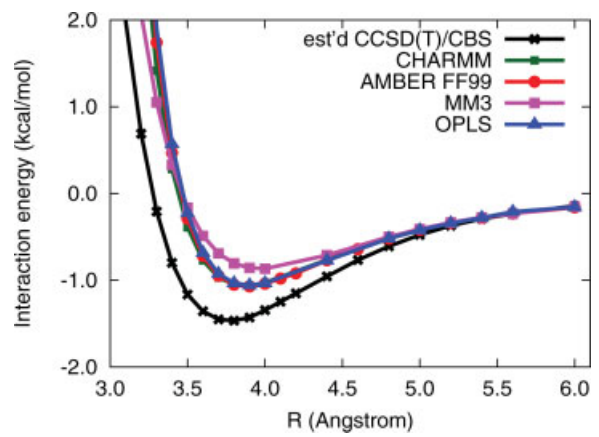

Figure 7. Interaction energy (kcal mol^{-1}) for the methane-benzene complex. Benchmark coupled-cluster data from Ref. 15.

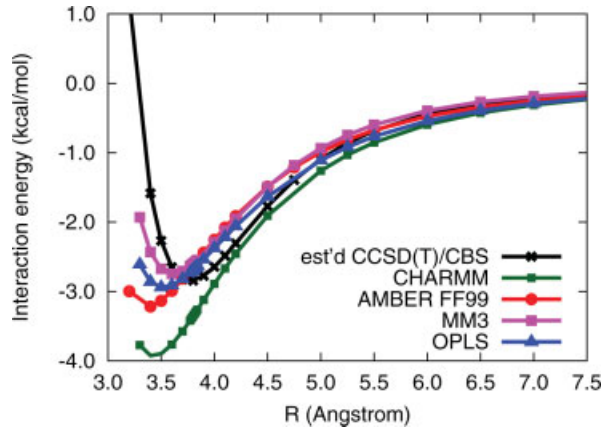

Figure 8. Interaction energy (kcal mol^{-1}) for the H_2S-benzene complex. Benchmark coupled-cluster data from Ref. 16.

to shorter distances compared to the benchmark curve. Perhaps surprisingly, MM3, which performed worst for the benzene dimer, now performs best for this test case.

The lack of consistency as the force fields are tested against various prototypes of noncovalent interactions means it is hard to recommend any of them as the best choice for general studies of more complex systems where nonbonded interactions are important. Although one could explore a more exhaustive comparison against a wider collection of benchmark-quality quantum data, the differences are large enough in some cases to raise the question about whether reliability could be substantially increased by an entirely new set of parameters, or whether the functional form of the force fields tested is simply too limited to allow much better agreement for a wide range of nonbonded interactions. Indeed, when one considers the simplicity of the empirical force fields and the fact that they were not parameterized using high-level quantum data, it is remarkable that they all provide good qualitative agreement and even semiquantitative agreement with the benchmark results.

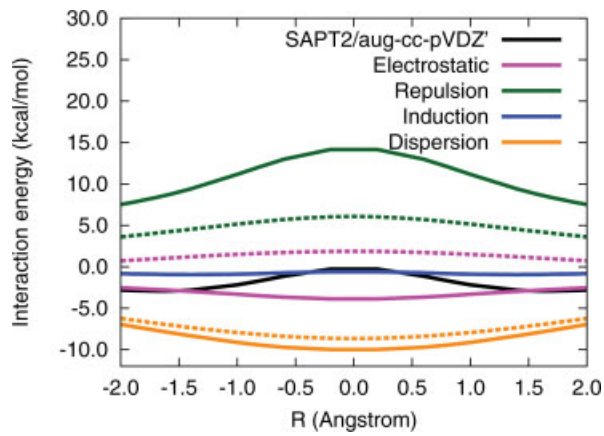

Figure 9. Interaction energy components (kcal mol^{-1}) for the parallel-displaced benzene dimer with a vertical interplanar separation of 3.4 Å. Solid lines represent components from SAPT2/aug-cc-pVDZ′ computations, and dashed lines are from CHARMM.

As an initial step toward addressing the question of whether standard functional forms are too simple to provide accurate results for non-bonded interactions, we have examined the benzene dimer in more detail to see whether different parameters might provide improved agreement with the quantum potential curves. The Lennard-Jones parameters and the unique atomic charge were then optimized by minimizing the absolute deviation between the CCSD(T)/CBS quantum interaction energies for the benzene dimer (including sandwich, T-shaped, and parallel-displaced configurations), with all data points weighted equally. All three vertical displacements for the parallel-displaced benzene dimer considered here (3.2, 3.4, and 3.6 Å) were included in the fit. During the optimization, parameters were allowed to vary from 0.5 to 2 times the CHARM27 values (better fits were obtained if these constraints were removed, but they led to unphysical parameter values). This process yields optimized Lennard-Jones parameters of ϵ(C) = 0.115, ϵ(H) = 0.011 kcal mol^{-1}, R_0(C) = 1.922, and R_0(H) = 1.230 Å, using the functional form of eq. (2). These compare to the CHARMM27 parameters of ϵ(C) = 0.070, ϵ(H) = 0.022 kcal mol^{-1} and R_0(C) = 1.9924, R_0(H) = 1.3200 Å for aromatic carbons and hydrogens. The corresponding AMBER parameters are ϵ(C) = 0.086, ϵ(H) = 0.015 kcal mol^{-1}, R_0(C) = 1.908, R_0(H) = 1.459 Å. The optimal charge was q(H) = −q(C) = 0.134 a.u. The results of this fit are presented in Figures 2–6 for the benzene dimer and are denoted "OPT-FF." The new parameters lead to modest overbinding near equilibrium for the sandwich configuration, but they improve significantly the underbinding of the empirical force fields for the T-shaped configuration. For parallel-displaced configurations, optimization of nonbonded parameters gives the empirical potential somewhat more curvature than some of the standard force fields, as desired; however, the improvement is small. Optimization shifts the potential curve so that it is approximately centered vertically with respect to the quantum potential. For vertical displacements of 3.2 or 3.4 Å, the curve is similar to that from AMBER, whereas for 3.6 Å it is somewhat more bound than AMBER, with smaller errors at larger horizontal displacements.

It would appear that the simple functional form of standard force fields with atom-centered charges is not sufficiently flexible to allow reliable modeling of noncovalent interactions in systems such as the parallel-displaced benzene dimer. To further explore this issue, we evaluated the components of the interaction energy for the parallel-displaced benzene dimer using symmetry-adapted perturbation theory[14] through second order (SAPT2), using the SAPT2006 program.[45] In keeping with our earlier work,[20] we have used a truncated basis set, denoted aug-cc-pVDZ′, which is the usual Dunning aug-cc-pVDZ basis[46,47] except that diffuse functions on hydrogen and diffuse *d* functions on carbon are neglected. This particular level of theory provides good agreement with the more accurate CCSD(T)/CBS data for interaction energies due to a favorable cancellation of errors.[48] It is possible that particular energy components are not fully converged at this level of theory; however, they should be accurate enough for the general discussion which follows.

Results of the SAPT2 analysis are plotted for a vertical interplanar separation of 3.4 Å in Figure 9 and compared to the corresponding electrostatic, dispersion, andshort-range repulsion terms from the CHARMM force field (because we did not use a polarizable force field, there are no induction terms in the force field). Although we focus on CHARMM for this comparison, qualitatively similar results would be observed for other force fields such as AMBER. The dispersion terms are fairly similar between SAPT2 and CHARMM, with the empirical dispersion term being slightly underestimated. However, the repulsion and electrostatic terms are very different. The repulsive term is greatly underestimated by CHARMM, and the electrostatic contribution is not nearly attractive enough. Presumably, the positive repulsion term in the Lennard-Jones function might be made more repulsive in an effort to match the SAPT2 exchange-repulsion energy. However, there is no straightforward way in which the point-charge electrostatic model might be made to agree with SAPT. Note that the quantum-mechanical electrostatic energy is (significantly) negative at all geometries shown, while in CHARMM it is always positive. This occurs because charge interpenetration (the overlap between the electron clouds of the two benzenes) makes a significant stabilizing contribution to the electrostatic energy[49,50] which is captured by SAPT2 but which cannot be captured by atom-centered charges or multipoles. Moreover, note that charge interpenetration means that the electrostatic energy is most stabilizing at horizontal displacements of zero (i.e., at the sandwich configuration). This is counter-intuitive and even impossible to describe using simple atom-centered point-charges, because in the sandwich configuration, all charges in one monomer are aligned directly above equal charges with the same sign in the other monomer. Because the electrostatic term is not stabilizing enough in the empirical force field, the repulsion energy must be underestimated to partially compensate for this error.

Although the induction contribution to the energy is by far the smallest, it is perhaps not completely negligible in this case. Although difficult to see from Figure 9, the induction contribution stabilizes the equilibrium configuration by more than 0.3 kcal mol^{-1} relative to the sandwich configuration, which is a significant fraction of the energy difference between CCSD(T)/CBS and CHARMM. For the smaller vertical displacement of 3.2 Å, this value grows to more than 0.7 kcal mol^{-1}. This suggests that polarization, in addition to more flexible electrostatic models, might be important in improving the reliability of empirical models for this test case.

Conclusions

Several popular empirical force fields have been compared against very high quality quantum mechanical potential curves for prototypes of π interactions. All of the empirical models demonstrate a correct qualitative and semiquantitative behavior, but none of those considered consistently reproduces the benchmark potentials. Moreover, the performance of the force fields is not consistent from one chemical system to the next. Even when the Lennard-Jones parameters are re-optimized to fit to the benzene dimer potentials, the resulting force field remains unable to provide a close fit to the quantum data, particularly for the parallel-displaced configurations. For nonpolarizable force fields such as those considered here, the gas-phase errors may partially compensate for the lack of polarization terms, which can be important in condensed phases; thus, the performance of these force fields can be expected to be somewhat better than suggested by the current gas-phase comparisons. However, the present analysis nevertheless suggests how force fields can be improved for π-interactions. An energy component analysis

using symmetry-adapted perturbation theory shows that improved agreement would require more flexible electrostatic models than the simple atom-centered point-charge model (specifically, those with some accounting of charge penetration effects), and that polarization terms can also be significant. The noncovalent systems considered here are recommended as test cases for the next-generation polarizable force fields that are being actively developed by a number of research groups. In future work, we plan to test the performance of several currently available polarizable force fields and improved electrostatic models.

Acknowledgments

The authors are grateful to Gregg Beckham (MIT) for sharing preliminary results from an independent attempt to fit force fields to our benzene dimer data, and they thank Anton Petrov (Georgia Tech) for helpful discussions.

References

1. Lehn, J.-M. Supramolecular Chemistry: Concepts and Perspectives; VCH: New York, 1995.
2. Diederich, F.; Künzer, H., Eds. Recent Trends in Molecular Recognition; Springer: New York, 1998.
3. Steed, J. W.; Atwood, J. L. Supramolecular Chemistry: A Concise Introduction; Wiley: New York, 2000.
4. Meyer, E. A.; Castellano, R. K.; Diederich, F. Angew Chem Int Ed Engl 2003, 42, 1210.
5. Saenger, W. Principles of Nucleic Acid Structure; Springer-Verlag: New York, 1984.
6. Burley, S. K.; Petsko, G. A. Science 1985, 229, 23.
7. Claessens, C. G.; Stoddart, J. F. J Phys Org Chem 1997, 10, 254.
8. Desiraju, G. R., Ed. Crystal Design: Structure and Function, volume 7 of Perspectives in Supramolecular Chemistry; Wiley: Hoboken, NJ, 2003.
9. Hunter, C. A. Angew Chem Int Ed Engl 1993, 32, 1584.
10. Hunter, C. A.; Sanders, J. K. M. J Am Chem Soc 1990, 112, 5525.
11. Sinnokrot, M. O.; Sherrill, C. D. J Phys Chem A 2003, 107, 8377.
12. Sinnokrot, M. O.; Sherrill, C. D. J Am Chem Soc 2004, 126, 7690.
13. Ringer, A. L.; Sinnokrot, M. O.; Lively, R. P.; Sherrill, C. D. Chem Eur J 2006, 12, 3821.
14. Jeziorski, B.; Moszynski, R.; Szalewicz, K. Chem Rev 1994, 94, 1887.
15. Ringer, A. L.; Figgs, M. S.; Sinnokrot, M. O.; Sherrill, C. D. J Phys Chem A 2006, 110, 10822.
16. Tauer, T. P.; Derrick, M. E.; Sherrill, C. D. J Phys Chem A 2005, 109, 191.
17. Leach, A. R. Molecular Modelling: Principles and Applications; 2nd ed.; Prentice Hall: Harlow, England, 2001.
18. Tsuzuki, S.; Honda, K.; Uchimaru, T.; Mikami, M.; Tanabe, K. J Am Chem Soc 2002, 124, 104.
19. Tsuzuki, S.; Uchimaru, T.; Sugawara, K.; Mikami, M. J Chem Phys 2002, 117, 11216.
20. Sinnokrot, M. O.; Sherrill, C. D. J Phys Chem A 2004, 108, 10200.
21. Řeha, D.; Kabeláč, M.; Ryjáček, F.; Šponer, J.; Šponer, J. E.; Elstner, M.; Suhai, S.; Hobza, P. J Am Chem Soc 2002, 124, 3366.
22. Jurečka, P.; Šponer, J.; Hobza, P. J Phys Chem B 2004, 108, 5466.
23. Macias, A. T.; MacKerell, A. D. J Comput Chem 2005, 26, 1452.
24. Ringer, A. L.; Senenko, A.; Sherrill, C. D. Protein Sci 2007, 16, 2216.
25. Jorgensen, W. J.; Maxwell, D. S.; Tirado-Rives, J. J Am Chem Soc 1996, 118, 11225.
26. Wang, J.; Cieplak, P.; Kollman, P. A. J Comput Chem 2000, 21, 1049.
27. Pearlman, D. A.; Case, D. A.; Caldwell, J. W.; Ross, W. S.; Cheatham, T. E.; DeBolt, S.; Ferguson, D.; Seibel, G.; Kollman, P. Comput Phys Commun 1995, 91, 1.
28. Brooks, B. R.; Bruccoleri, R. E.; Olafson, B. D.; States, D. J.; Swaminathan, S.; Karplus, M. J Comput Chem 1983, 4, 187.
29. Jorgensen, W. L.; Tirado-Rives, J. J Am Chem Soc 1988, 110, 1657.
30. Kaminski, G. A.; Friesner, R. A.; Tirado-Rives, J.; Jorgensen, W. J. J Phys Chem B 2001, 105, 6474.
31. Allinger, N. L.; Yuh, Y. H.; Lii, J.-H. J Am Chem Soc 1989, 111, 8551.
32. Repasky, M. P.; Chandrasekhar, J.; Jorgensen, W. L. J Comput Chem 2002, 23, 1601.
33. Stewart, J. J. P. J Comput Chem 1989, 10, 209.
34. Walker, R. C.; Crowley, M. F.; Case, D. A. J Comput Chem 2008, 29, 1019.
35. Cornell, W. D.; Cieplak, P.; Bayly, C. I.; Gould, I. R.; Kerz, K. M.; Ferguson, D. M.; Spellmeyer, D. C.; Fox, T.; Caldwell, J. W.; Kollman, P. A. J Am Chem Soc 1995, 117, 5179.
36. Jorgensen, W. L.; Severance, D. L. J Am Chem Soc 1990, 112, 4768.
37. Ren, P.; Ponder, J. W. J Phys Chem B 2003, 107, 5933.
38. Ren, P.; Ponder, J. W. J Comput Chem 2002, 23, 1497.
39. Ponder, J. W.; Richards, F. M. J Comput Chem 1987, 8, 1016.
40. MacKerell, A. D.; Wiórkiewicz-Kuczera, Karplus, M. J Am Chem Soc 1995, 117, 11946.
41. MacKerell, A. D.; Bashford, D.; Bellott, M.; Dunbrack, R. L.; Evanseck, J. D.; Field, M. J.; Fischer, S.; Gao, J.; Guo, H.; Ha, S.; Joseph-McCarthy, D.; Kuchnir, L.; Kuczera, K.; Lau, F. T. K.; Mattos, C.; Michnick, S.; Ngo, T.; Nguyen, D. T.; Prodhom, B.; Reiher, W. E.; Roux, B.; Schlenrich, M.; Smith, J. C.; Stote, R.; Straub, J.; Watanabe, M.; Wiórkiewicz-Kuczera, J.; Yin, D.; Karplus, M. J Phys Chem B 1998, 102, 3586.
42. Foloppe, N.; MacKerell, A. D. J Comput Chem 2000, 21, 86.
43. Case, D. A.; Darden, T. A.; Cheatham, T. E.; Simmerling, C. L.; Wang, J.; Duke, R. E.; Luo, R.; Merz, K. M.; Pearlman, D. A.; Crowley, M.; Walker, R. C.; Zhang, W.; Wang, B.; Hayik, S.; Roitberg, A.; Seabra, G.; Wong, K. F.; Paesani, F.; Wu, X.; Brozell, S.; Tsui, V.; Gohlke, H.; Yang, L.; Tan, C.; Mongan, J.; Hornak, V.; Cui, G.; Beroza, P.; Mathews, D. H.; Schafmeister, C.; Ross, W. S.; Kollman, P. A. AMBER 9, University of California, San Francisco, 2006.
44. Crawford, T. D.; Sherrill, C. D.; Valeev, E. F.; Fermann, J. T.; King, R. A.; Leininger, M. L.; Brown, S. T.; Janssen, C. L.; Seidl, E. T.; Kenny, J. P.; Allen, W. D. J Comput Chem 2007, 28, 1610.
45. Bukowski, R.; Cencek, W.; Jankowski, P.; Jeziorski, B.; Jeziorska, M.; Kucharski, S. A.; Lotrich, V. F.; Misquitta, A. J.; Moszynski, R.; Patkowski, K.; Rybak, S.; Szalewicz, K.; Williams, H. L.; Wheatley, R. J.; Wormer, P. E. S.; Zuchowski, P. S. SAPT2006: An ab initio program for many-body symmetry-adapted perturbation theory calculations of intermolecular interaction energies. Available at: http://www.physics.udel.edu/∼szalewic/SAPT.
46. Dunning, T. H. J Chem Phys 1989, 90, 1007.
47. Kendall, R. A.; Dunning, T. H.; Harrison, R. J. J Chem Phys 1992, 96, 6796.
48. Sinnokrot, M. O.; Sherrill, C. D. J Phys Chem A 2006, 110, 10656.
49. Stone, A. J. The Theory of Intermolecular Forces; Oxford University Press: Oxford, 1996.
50. Kairys, V.; Jensen, J. H. Chem Phys Lett 1999, 315, 140.